RESEARCH BRIEF

Overcoming PD-1 Blockade Resistance with CpG-A Toll-Like Receptor 9 Agonist Vidutolimod in Patients with Metastatic Melanoma

Antoni Ribas[1], Theresa Medina[2], John M. Kirkwood[3], Yousef Zakharia[4], Rene Gonzalez[2], Diwakar Davar[3], Bartosz Chmielowski[1], Katie M. Campbell[1], Riyue Bao[3], Heather Kelley[5], Aaron Morris[5], David Mauro[5], James E. Wooldridge[5], Jason J. Luke[3], George J. Weiner[4], Arthur M. Krieg[5], and Mohammed M. Milhem[4]

ABSTRACT Patients with advanced melanoma that is resistant to PD-1 blockade therapy have limited treatment options. Vidutolimod (formerly CMP-001), a virus-like particle containing a CpG-A Toll-like receptor 9 (TLR9) agonist, may reverse PD-1 blockade resistance by triggering a strong IFN response to induce and attract antitumor T cells. In the dose-escalation part of this phase Ib study, vidutolimod was administered intratumorally at escalating doses with intravenous pembrolizumab to 44 patients with advanced melanoma who had progressive disease or stable disease on prior anti–PD-1 therapy. The combination of vidutolimod and pembrolizumab had a manageable safety profile, and durable responses were observed in 25% of patients, with tumor regression in both injected and noninjected lesions, including visceral lesions. Patients who responded to vidutolimod and pembrolizumab had noninflamed tumors at baseline and induction of an IFNγ gene signature following treatment, as well as increased systemic expression of the IFN-inducible chemokine CXCL10.

SIGNIFICANCE: In this phase Ib study in patients with advanced melanoma, intratumoral TLR9 agonist vidutolimod in combination with pembrolizumab had a manageable safety profile and showed promising clinical activity, supporting the further clinical development of vidutolimod to overcome PD-1 blockade resistance through induction of an IFN response.

See related commentary by Sullivan, p. 2960.

INTRODUCTION

Tumors that contain CD8$^+$ T cells and express an IFN response signature, including PD-L1 expression, are most likely to regress following single-agent PD-1 blockade (1–4), and type I IFN response is essential for induction of antitumor immunity (5). The major innate immune cells producing type I IFN in response to viral infection are plasmacytoid

[1]University of California, Los Angeles, Los Angeles, California. [2]University of Colorado Cancer Center, Aurora, Colorado. [3]University of Pittsburgh, UPMC Hillman Cancer Center, Pittsburgh, Pennsylvania. [4]University of Iowa, Iowa City, Iowa. [5]Checkmate Pharmaceuticals, Inc., Cambridge, Massachusetts.

Current address for H. Kelley: Checkmate Pharmaceuticals, Inc., Cambridge, Massachusetts (as an independent contractor); current address for D. Mauro: Prelude Therapeutics, Inc., Wilmington, Delaware.

Corresponding Author: Antoni Ribas, Jonsson Comprehensive Cancer Center, University of California, Los Angeles, 11-934 Factor Building, 10833 Le Conte Avenue, Los Angeles, CA 90095. Phone: 310-206-3928; Fax: 310-825-2493; E-mail: aribas@mednet.ucla.edu

Cancer Discov 2021;11:2998–3007

doi: 10.1158/2159-8290.CD-21-0425

dendritic cells (pDC), which express Toll-like receptor 7 (TLR7) and TLR9 (6, 7) and are frequently present in tumors in an inactivated state (6, 7). TLR7 can be activated by most RNA sequences, whereas TLR9 is specifically activated by unmethylated CpG dinucleotides, which are prevalent in the genomes of pathogens (7, 8). Intratumoral injection of TLR agonists could induce an IFN response signature and antitumor $CD8^+$ T cells, thereby improving responses to PD-1 blockade. As TLR9-mediated T-cell activation can induce PD-1 expression (9), combining TLR9 agonists with approved PD-1 blockade therapies is a rational approach to target cancer immune evasion.

CpG-A, CpG-B, and CpG-C oligodeoxynucleotides are the three major classes of TLR9 agonists and differ in their molecular structures, endosomal trafficking, downstream TLR9 signaling, and patterns of pDC activation (8, 10). CpG-A oligodeoxynucleotides induce the strongest differentiation of pDCs into the transcriptionally distinct P1 subset, which is primarily responsible for the type I IFN response (11). CpG-A oligodeoxynucleotides have been shown to activate tumor-associated pDCs to secrete type I IFNs and stimulate $CD4^+$ and $CD8^+$ T cells *in vitro* (6). Furthermore, pDC activation by nucleic acids can be greatly enhanced when the nucleic acids are contained within immune complexes resulting in the costimulation of CD32 (Fcγ receptor II), which is also expressed on pDCs (12, 13).

Vidutolimod (formerly termed CMP-001, CYT003, or QbG10) is a CpG-A oligodeoxynucleotide packaged within a virus-like particle (VLP) formed by a bacteriophage coat protein, Qβ (14). In preclinical studies, vidutolimod induced anti-Qβ antibody production after the first dose, and, upon subsequent injections, these antibodies formed immune complexes with the VLP to facilitate pDC uptake and activation through CD32 (14). In a mouse model, intratumoral injection of vidutolimod induced similar local tumor regression but greater systemic tumor regression than naked CpG-A (14), suggesting that costimulation of TLR9 and CD32 may improve cancer immunotherapy outcomes. The benefit of intratumoral delivery is selective activation of tumor-associated pDCs that can present tumor antigens to $CD8^+$ T cells, driving a specific antitumor response. In addition, local administration allows a reduction in the amount of drug used, thereby reducing systemic exposure and limiting off-target toxicities. Furthermore, intratumoral strategies have the potential to overcome resistance to single-agent PD-1 blockade by converting uninflamed tumor microenvironments (TME) into inflamed TME, locally priming T cells and/or allowing their intratumoral homing. In this phase Ib study, we evaluated intratumoral vidutolimod in combination with systemic anti–PD-1 therapy to overcome PD-1 blockade resistance in patients with advanced melanoma.

RESULTS

Patient Characteristics

Between April 14, 2016, and June 14, 2017, 44 patients with advanced melanoma previously treated with anti–PD-1 therapy were enrolled at four academic institutions in the dose-escalation phase of this study. The median time of all prior anti–PD-1 treatments was 5 months (range, 1.1–29.9 months), and 61% of patients (27/44) received their last prior anti–PD-1 treatment within 2 months of their first dose of vidutolimod and pembrolizumab. At the time of study entry, 91% of patients (40/44) had progressive disease (PD) as their last response to prior anti–PD-1 therapy; the remaining patients had stable disease (SD; 2/44) or unknown response (2/44; Table 1). Seven percent of patients (3/44) had melanoma confined to the skin, 30% (13/44) had soft tissue and/or lymph node involvement, and the remaining 64% (28/44) had bone and/or visceral metastases (Supplementary Table S1). Vidutolimod injection sites included skin, lymph nodes, soft tissue, and, in one patient, a liver metastasis. No major differences were observed between vidutolimod dosing schedule A ($n = 31$) and B ($n = 13$; Supplementary Fig. S1) with respect to demographics, baseline characteristics, adverse events (AE), or treatment response; therefore, these schedules were pooled for analysis. At the time of data cutoff (May 8, 2020), one patient remained on study treatment. The other patients discontinued the study due to PD [52% (23/44)], consent withdrawal per investigator reporting [23% (10/44)], investigator decision [18% (8/44)], or treatment-related adverse events [TRAE; 5% (2/44); Supplementary Fig. S1]. Among the patients withdrawing consent, one patient stopped after their initial complete response (CR) assessment and maintained a CR for at least another 22 months, and four patients had PD prior to study discontinuation.

Safety

Patients received a median of 8 vidutolimod injections (range, 2–48) and a median of 5.5 pembrolizumab doses (range, 1–52). All patients received pembrolizumab at 2 mg/kg intravenously every 3 weeks (Q3W); four patients also received at least two 200-mg doses. Two patients discontinued treatment because of TRAEs, and two discontinued because of AEs related to PD. Supplementary Table S2 reports the incidence of AEs of any grade regardless of attribution to PD or study treatment. One patient had fatal respiratory failure, which was considered unrelated to study treatment. AEs attributed to the study treatment are reported in Supplementary Table S3. Grade 3/4 TRAEs occurred in 20 patients (45%); incidence was highest following the third injection of vidutolimod (initial weekly injection phase) and declined in frequency and severity after the sixth injection and during subsequent Q3W dosing (Supplementary Fig. S2). No grade 5 TRAEs occurred. The most common TRAEs (≥25%) were flu-like symptoms (chills, fever, nausea, fatigue, vomiting, headache, and diarrhea), hypotension, injection site pain, and arthralgia, which are expected side effects with the activation of pattern-recognition receptors. The most commonly reported grade 3/4 TRAE was hypotension [16%; grade 3 ($n = 6$); grade 4 ($n = 1$)]. There was no apparent dose relationship in the severity or incidence of all-cause AEs or TRAEs (Supplementary Tables S2 and S3).

Antitumor Activity

Eleven of the 44 patients [25%; 95% confidence interval (CI), 13%–40%] achieved a partial response (PR) or CR when assessed using Response Evaluation Criteria In Solid Tumors version 1.1 (RECIST v1.1; Table 2; Fig. 1A). Four patients had a CR and seven patients had a PR. Of these responders, one patient had a last response of SD and 10 patients had a

Table 1. Patient demographics and baseline characteristics[a]

Demographic or baseline characteristics	Vidutolimod 1-mg Cohort (*n* = 3)	Vidutolimod 3-mg Cohort (*n* = 16)	Vidutolimod 5-mg Cohort (*n* = 9)	Vidutolimod 7.5-mg Cohort (*n* = 6)	Vidutolimod 10-mg Cohort (*n* = 10)	All patients (*N* = 44)
Median age, years (range)	68 (68–80)	63 (45–75)	55 (33–77)	71 (48–83)	64 (35–86)	64 (33–86)
Male, *n* (%)	3 (100)	6 (38)	5 (56)	4 (67)	5 (50)	23 (52)
ECOG PS, *n* (%)						
0	2 (67)	9 (56)	6 (67)	4 (67)	8 (80)	29 (66)
1	1 (33)	7 (44)	3 (33)	2 (33)	2 (20)	15 (34)
BRAF^{V600E}-positive, *n* (%)	0	5 (31)	3 (33)	2 (33)	6 (60)	16 (36)
Received prior BRAF/MEK inhibitor	0	3 (19)	1 (11)	0	2 (20)	6 (14)
LDH levels,[b] *n* (%)						
Normal/low	0	11 (69)	9 (100)	3 (50)	6 (60)	29 (66)
High	0	5 (31)	0	3 (50)	4 (40)	12 (27)
Unknown	3 (100)	0	0	0	0	3 (7)
Prior therapies,[c] *n*, median (range)	2 (1–5)	4 (1–8)	2 (1–8)	1.5 (1–3)	1 (1–4)	2 (1–8)
1, *n* (%)	1 (33)	2 (13)	3 (33)	3 (50)	6 (60)	15 (34)
2–3, *n* (%)	1 (33)	5 (31)	4 (44)	3 (50)	3 (30)	16 (36)
≥4, *n* (%)	1 (33)	9 (56)	2 (22)	0	1 (10)	13 (30)
Prior checkpoint inhibitor therapies received, *n* (%)						
Any anti–PD-1 monotherapy	2 (67)	14 (88)	8 (89)	5 (83)	4 (40)	33 (75)
Any anti–PD-1 combination therapy	1 (33)	7 (44)	4 (44)	1 (17)	6 (60)	19 (43)
Prior anti–PD-1 therapy best response, *n* (%)						
CR	0	0	0	1 (17)	1 (10)	2 (5)
PR	0	0	1 (11)	0	0	1 (2)
SD	2 (67)	5 (31)	3 (33)	2 (33)	2 (20)	14 (32)
PD	0	9 (56)	5 (56)	3 (50)	5 (50)	22 (50)
Unknown	1 (33)	2 (13)	0	0	2 (20)	5 (11)
Prior anti–PD-1 therapy last response, *n* (%)						
SD	0	1 (6)	1 (11)	0	0	2 (5)
PD	2 (67)	14 (88)	8 (89)	6 (100)	10 (100)	40 (91)
Unknown	1 (33)	1 (6)	0	0	0	2 (5)

Abbreviation: LDH, lactate dehydrogenase.

[a]All patients across all dose cohorts were of white race.

[b]Out-of-range values defined by site normal ranges.

[c]Prior therapies exclude radiation and surgeries/excisions.

last response of PD to prior anti–PD-1 therapy. All responses were confirmed except for two PRs. In responding patients, target lesions showed progressive reductions in tumor volume, suggesting that responses deepened over time (Fig. 1B). Median duration of response (DOR) per RECIST v1.1 was 19.5 months (95% CI, 5.8–not estimable), including 5 patients with responses >23 months (Fig. 1C). Median time to response was 2.5 months (range, 1.9–5.8), and median progression-free survival (PFS) was 2.8 months (95% CI, 2.7–5.4). Responses were also observed in patients receiving on-study steroids (Supplementary Table S4) and in patients with various baseline disease sites (Supplementary Table S2). Using modified RECIST v1.1 for immune-based therapeutics (iRECIST; ref. 15) assessed by blinded central review, there were two additional patients with a response to therapy (Supplementary Fig. S3A and S3B), one of whom had experienced PD on treatment with a different TLR9 agonist (SD-101; CpG-C oligodeoxynucleotide) and pembrolizumab.

Vidutolimod-injected and noninjected target lesions, including visceral metastases, demonstrated similar tumor volume reductions (Supplementary Fig. S4). Complete regression of two injected scalp metastases was observed in a 77-year-old man who experienced PD on prior pembrolizumab monotherapy (Fig. 1D). This patient was previously treated with pembrolizumab for 1 month (best response of PD), with 2 months elapsing from the last pembrolizumab dose to the start of vidutolimod study treatment. Radiologic imaging from two other heavily pretreated patients demonstrated systemic responses in noninjected lesions (Fig. 1E and F; prior therapies and best/last response assessment available in Supplementary Material). A 48-year-old woman who was previously treated with pembrolizumab for 2.5 months, with

Table 2. Clinical response with vidutolimod in combination with pembrolizumab

	Vidutolimod					
	1-mg Cohort ($n=3$)	3-mg Cohort ($n=16$)	5-mg Cohort ($n=9$)	7.5-mg Cohort ($n=6$)	10-mg Cohort ($n=10$)	All patients ($N=44$)
ORR,[a] *n* (%)	0	3 (19)	4 (44)	0	4 (40)	11 (25)
(95% CI)	(0–71)	(4–46)	(14–79)	(0–46)	(12–74)	(13–40)
CR	0	1 (6)	2 (22)	0	1 (10)	4 (9)
PR	0	2 (13)	2 (22)	0	3 (30)	7 (16)
SD	0	1 (6)	2 (22)	2 (33)	2 (20)	7 (16)
PD	3 (100)	10 (63)	2 (22)	4 (67)	3 (30)	22 (50)
Unknown[b]	0	2 (13)	1 (11)	0	1 (10)	4 (9)

Abbreviation: ORR, objective response rate.

[a]ORR per RECIST v1.1 as assessed by the investigator.

[b]Four patients discontinued study prior to having follow-up scans.

8 months elapsing from the last dose of pembrolizumab to the start of vidutolimod study treatment, had regression of visceral lung metastases (noninjected target lesions) following injection of an inguinal lymph node (Fig. 1E). A 46-year-old woman who was previously treated with pembrolizumab for 1 month, with 2 months elapsing from the last dose of pembrolizumab to the start of vidutolimod study treatment, had regression of noninjected liver and groin metastases (Fig. 1F). On the basis of emerging data and the absence of dose-limiting toxicities or a clear dose response, vidutolimod 10 mg was selected as the dose for further clinical development.

In Vitro Induction of Cytokine Secretion with Vidutolimod

In vitro culture of normal human peripheral blood mononuclear cells (PBMC) with a panel of innate immune activators demonstrated that vidutolimod had the greatest IFNα induction compared with CpG-B or CpG-C TLR9 agonists, as well as other TLR agonists, including agonists of TLR4 and TLR7/8 (Supplementary Fig. S5A). Similar levels of IFNα induction were observed for both the naked CpG-A oligodeoxynucleotide contained within the VLP in vidutolimod (G10) and for vidutolimod (G10 within the VLP) immune complexes (plus anti-Qβ antibodies required for VLP opsonization and cellular uptake). The TLR4 and TLR7/8 agonists resulted in the strongest induction of IL6, a proinflammatory cytokine implicated in AEs, including cytokine release syndromes (16), compared with all TLR9 agonists assessed (Supplementary Fig. S5B), whereas the TLR7/8 agonist resulted in the strongest induction of IL10, an anti-inflammatory cytokine (Supplementary Fig. S5C).

In Vivo Anti-Qβ Antibody and Serum Chemokine Induction

C-X-C motif chemokine ligand 10 (CXCL10), a type I IFN–induced chemokine that mediates T-cell migration, served as the primary pharmacodynamic marker for TLR9-induced pDC activation *in vivo* (17). High concentrations of anti-Qβ antibodies to the immunogenic VLP were observed in all patients within 2 weeks of initial vidutolimod exposure (Supplementary Fig. S6A and S6B), as expected (18). Serum CXCL10 levels did not increase significantly following the first vidutolimod injection (i.e., before induction of anti-Qβ antibodies; Fig. 2A). However, CXCL10 levels increased as early as 2 hours and peaked at 24 hours following the third and subsequent vidutolimod injections (Fig. 2A). Furthermore, a trend toward higher serum levels of CXCL10, but not IL6, was observed in patients with CR/PR/SD versus PD (not statistically significant; Fig. 2B and C).

Markers of Tumor Inflammation Before and After Vidutolimod Injection

Antitumor CD8$^+$ T cells induced upon TLR9 activation express PD-1 (14), thus providing a rationale for combining PD-1 blockade with TLR9 agonists to improve the durability of clinical responses. Therefore, we assessed baseline and on-treatment biopsies from this study for markers of T-cell activation. Adequate baseline archival or fresh tumor biopsies were available from 22 patients, five of whom also provided on-treatment biopsies. Baseline tumor biopsies generally contained low CD8$^+$ T-cell infiltration, PD-L1 expression, and IFNγ-related gene expression (Fig. 2D; refs. 19, 20). On-treatment biopsies of injected lesions from patients with PD had no evidence of TLR9 activation (Fig. 2E). On-treatment biopsies of an injected lesion from a patient with PD and an injected and a noninjected lesion from a patient with PR showed increased CD8$^+$ T-cell infiltration, PD-L1 expression, and expression of IFNγ-related genes compared with baseline (Fig. 2E).

DISCUSSION

The advent of PD-1 blockade dramatically changed the treatment paradigm across different tumor types, including melanoma. Unfortunately, many patients do not achieve a meaningful antitumor response, and established therapies to overcome primary or secondary resistance to PD-1 blockade are lacking (21). In this study in patients with melanoma, the combination of intratumoral vidutolimod and intravenous pembrolizumab demonstrated a manageable safety profile

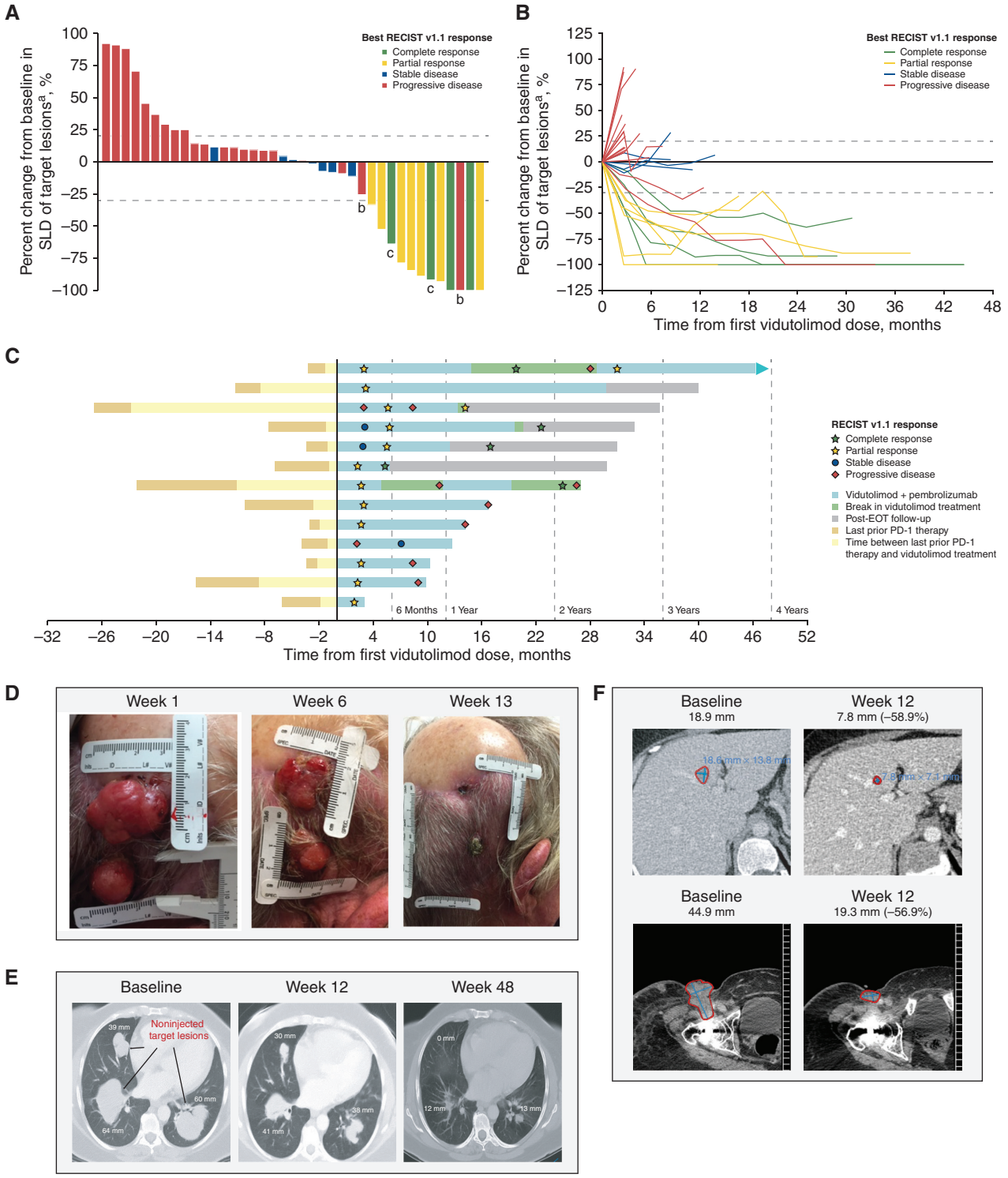

Figure 1. Antitumor activity of vidutolimod plus pembrolizumab. **A,** Best percent change in SLD of target lesions from baseline. **B,** Percent change from baseline in SLD of target lesions over time. The bars (**A**) and lines (**B**) are colored on the basis of best overall response by RECIST v1.1 as determined by the investigator. **C,** Duration of vidutolimod treatment, onset, and DOR for each patient with a RECIST v1.1 response ($n = 11$) and patients with an iRECIST response ($n = 2$). RECIST v1.1 disease status shown was based on investigator assessment. Representative photographs (**D**) and radiologic imaging (**E** and **F**) demonstrating tumor regression of two injected scalp metastases (**D**), noninjected visceral lung metastases (**E**), and noninjected liver (**F**, top) and groin (**F**, bottom) metastases from three different patients. [a]Five patients with missing or incomplete postbaseline disease assessments were not included. [b]Patients had initial PD per RECIST v1.1 and were later shown to have a PR per iRECIST as determined by blinded central review ($n = 2$). [c]Patients with CR had less than 100% target lesion regression (target lymph nodes were less than 1.0 cm in diameter and met the RECIST v1.1 definition of CR). EOT, end of treatment; SLD, sum of longest diameters.

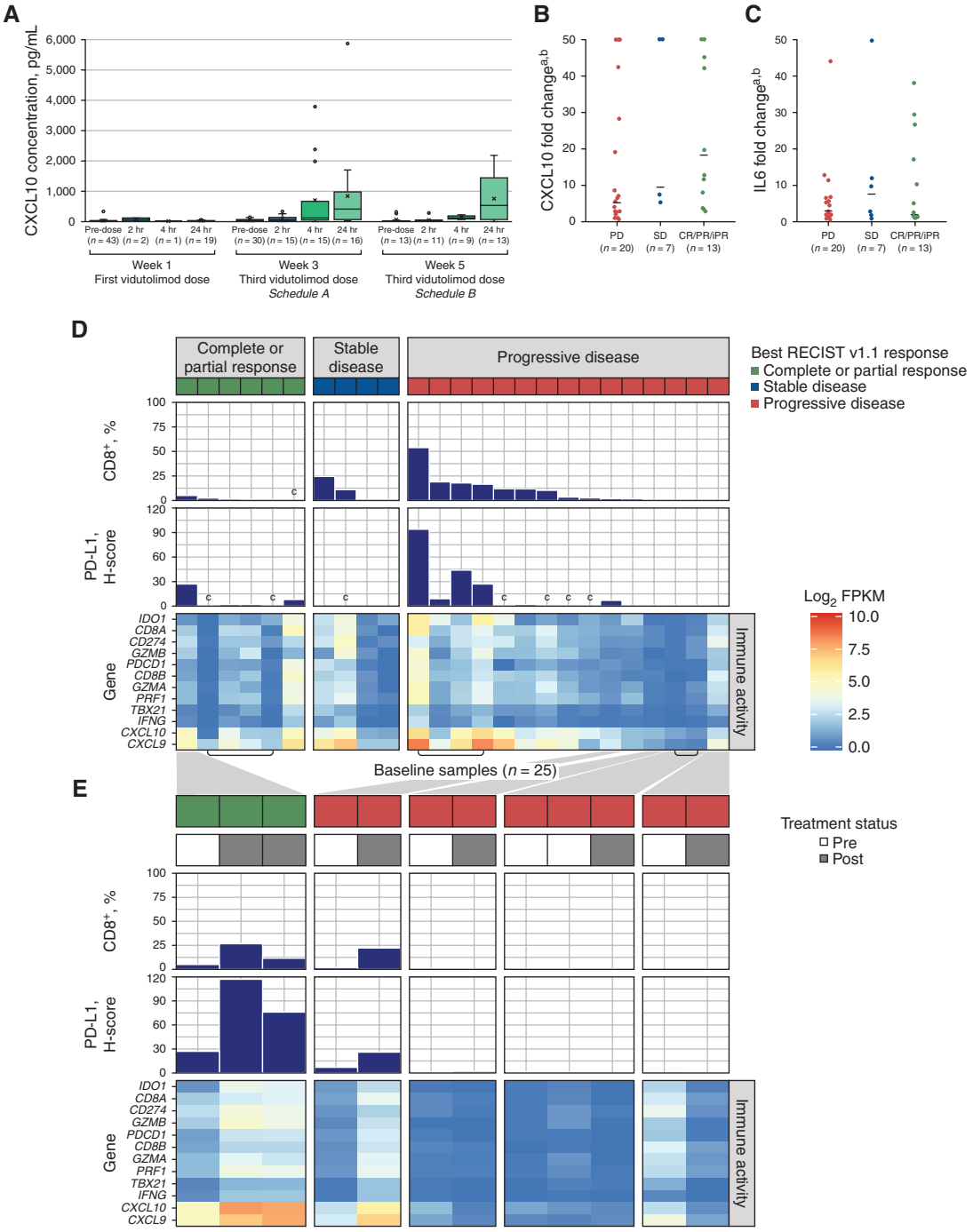

Figure 2. Chemokine induction and transcriptomic analyses. **A,** Box and whisker plot of serum CXCL10 concentrations preinjection and 2, 4, and 24 hours postinjection after the first vidutolimod injection and the third vidutolimod injection (schedule A, week 3; schedule B, week 5). Mean values are indicated by "x" symbols and outliers are shown as circles. The fold change in CXCL10 (**B**) and IL6 (**C**) at 24 hours from baseline across response groups. Both RECIST v1.1 responders ($n = 11$) and iRECIST responders ($n = 2$) are included in the CR/PR/iPR group. Horizontal lines indicate median values. **D,** Heat map of gene expression across genes associated with the IFNγ pathway and immune cell infiltration for 25 baseline samples taken from 22 patients. Three patients had two available biopsy samples each (archival and baseline) and both were analyzed (indicated by brackets underneath the heat map). Samples (*x*-axis) were sorted by decreasing frequency of $CD8^+$ T cells in the full tissue (measured by IHC; bar chart) and by RECIST v1.1 best overall response (colored bars across the top of the figure). PD-L1–positive full tissue H-score is also shown (measured by IHC). **E,** Heat map of gene expression across paired baseline and on-study tumor biopsies as indicated by pretreatment and posttreatment bars (gray/white) across the top of the figure for 12 biopsies taken from five patients. The responding patient on the left had two posttreatment biopsies; the left biopsy was taken from an injected lesion, and the right biopsy was taken from a noninjected lesion. All other posttreatment biopsies were taken from injected lesions. Gray shading is used to indicate the patient identity between **D** and **E**. [a]Below quantitation limit values were set to the lower limit of quantitation and above quantitation limit values were set to the upper limit of quantitation. [b]Values capped at 50 for plotting purposes. [c]Inadequate samples for this metric. FPKM, fragments per kilobase of transcript per million mapped reads; H-score, histology score; iPR, PR by iRECIST; SD, standard deviation.

and promising clinical activity to overcome PD-1 blockade resistance by inducing durable regression of both injected and distant, noninjected tumors, including visceral metastases. With an objective response rate (ORR) of 25% per RECIST v1.1, the response rate of vidutolimod plus pembrolizumab in this heavily pretreated patient population was substantially higher than the response rates observed in patients treated with PD-1 blockade beyond initial progression (6%–7%; ref. 22) and in line with response rates observed with other anti–PD-1 combinations as second-line treatments (23). Reports of response rates with PD-1 blockade retreatment in later lines of therapy are scarce. On the basis of a limited number of biopsies, tumors in patients with responses were generally noninflamed at baseline, which may have contributed to the patients' progression on prior anti–PD-1 therapy (1, 3, 4). Intratumoral injection of vidutolimod induced IFN-mediated tumor inflammation, as demonstrated by increased $CD8^+$ T-cell numbers, PD-L1 expression, and IFNγ gene signature, in injected and noninjected lesions of the only responder with available baseline and on-treatment biopsies. In contrast, patients with PD showed a trend toward lower induction of IFN-regulated serum CXCL10 compared with patients with CR/PR/SD, and three of four patients with PD and baseline and on-treatment biopsies showed no increase in tumor IFNγ gene signature.

Previous studies have demonstrated tumor regression in patients with non-Hodgkin lymphoma following intratumoral administration of a CpG-B oligodeoxynucleotide (24) and in patients with advanced melanoma treated with intratumoral administration of the CpG-C oligodeoxynucleotide SD-101 in combination with intravenous pembrolizumab, including 2 of 13 patients who had progression on prior anti–PD-1 therapy (25). However, a phase III trial of the CpG-C oligodeoxynucleotide tilsotolimod in combination with ipilimumab recently failed to improve survival in advanced PD-1 blockade–refractory melanoma (https://ir.iderapharma.com/news-releases/news-release-details/idera-pharmaceuticals-announces-results-illuminate-301-trial). This lack of confirmed efficacy may be driven by insufficient clinical activity of the TLR9 agonist or the checkpoint inhibitor used in the combination. In contrast to SD-101 and tilsotolimod, vidutolimod is a CpG-A oligodeoxynucleotide that induces a distinct pattern of pDC differentiation, leading to a much greater magnitude of type I IFN secretion, and greater stimulation of $CD4^+$ and $CD8^+$ T cells *in vitro* (6, 11). Vidutolimod's activity is further enhanced by its delivery within the Qβ VLP, which triggers an anti-Qβ antibody response that provides immune complex–mediated costimulation of CD32 (Fcγ receptor II; refs. 12, 13). The cell population targeted by anti-Qβ–coated vidutolimod is broader than that targeted by TLR9 agonist alone (26). *In vitro*, anti-Qβ–coated vidutolimod altered the response of TLR9-negative myeloid cells to cytokines (26). This altered response to cytokines may contribute to an enhanced antitumor response with vidutolimod. Consistent with these key distinguishing features, vidutolimod is the only TLR9 agonist that has shown clinical activity as a single agent in patients with advanced anti–PD-1–refractory melanoma (27). Lastly, it may be critical to use an anti–PD-1 agent in combination with a TLR9 agonist to counteract the effects of PD-L1 upregulation and allow for the sustained activity of antitumor $CD8^+$ T cells activated by the TLR9 agonist. Our results demonstrate the ability to durably overcome PD-1 blockade resistance with a VLP-encapsulated CpG-A TLR9 agonist in combination with pembrolizumab. These data are also consistent with the hypotheses that (i) in responding patients with advanced melanoma, intratumoral vidutolimod activates tumor-associated pDCs to secrete type I IFN, which induces Th1 antitumor immunity manifested by the rapid production of CXCL10 and the subsequent generation of IFNγ-secreting $CD8^+$ T cells; and (ii) nonresponding tumors may have primary resistance to TLR9 activation in tumor-associated pDCs, similar to observations in several other advanced cancers (6, 7). The promising clinical activity observed in this phase Ib study supports combining the potent CpG-A TLR9 agonist vidutolimod with PD-1 blockade as a rational approach to target cancer immune evasion. Clinical studies have been initiated to confirm the safety and efficacy of vidutolimud in combination with PD-1 blockade in previously untreated patients with melanoma (NCT04695977) and in patients with PD-1 blockade–resistant melanoma (NCT04698187).

METHODS

Patients

Eligible patients were age ≥18 years, had histologically confirmed metastatic nonuveal melanoma, had metastatic lesions amenable to intralesional injection, and had current or previous treatment with any anti–PD-1/PD-L1 at time of study enrollment; patients with current treatment must have had SD per RECIST v1.1 after ≥12 weeks (≥4 doses), or must have had PD per RECIST v1.1 on treatment; patients with previous treatment (anti–PD-1/PD-L1 alone or in combination) must have been deemed to have not responded to this therapy/combination, irrespective of the timing of the prior therapy relative to first dose of vidutolimod. PD-1 blockade was not required to be the last treatment prior to study entry. Patients were required to have measurable disease per RECIST v1.1 and Eastern Cooperative Oncology Group performance status of 0 or 1. Key exclusion criteria included anti-CTLA4 or investigational therapy administered within 30 days, requirement of systemic corticosteroids >10 mg per day prednisone equivalent, prior grade 4 autoimmune toxicities resulting from prior immunotherapy, or known active central nervous system metastases.

The study protocol and its amendments were approved by the relevant institutional review boards, and the study was conducted in accordance with the Declaration of Helsinki and the International Conference on Harmonisation Guidelines for Good Clinical Practice. All patients signed written informed consent prior to receiving study treatment.

Study Design and Treatment

The dose-escalation part of this open-label, multicenter, phase Ib study (NCT03084640) of vidutolimod in combination with pembrolizumab followed a 3+3 design. Vidutolimod (1, 3, 5, 7.5, or 10 mg) was injected intratumorally into ≥1 lesion weekly for 7 weeks, followed by Q3W thereafter (schedule A); or weekly for 2 weeks, followed by Q3W thereafter (schedule B). Investigators were advised to use their discretion to identify and inject the most aggressively growing accessible lesion; the total dose of vidutolimod could be split among several lesions. If the injected tumors regressed or if a new lesion appeared, the investigator could inject another accessible tumor; if no accessible lesions remained, the investigator could inject vidutolimod subcutaneously in the area of former disease. Pembrolizumab was administered intravenously according to the Keytruda (pembrolizumab) prescribing information. Study treatment could

be discontinued because of PD, unacceptable toxicity, investigator decision, or withdrawal of consent. Patients with PD could continue study therapy at the discretion of the investigator.

Premedications, including antipyretics, antiemetics, and intravenous fluids, were recommended but not required. A subsequent protocol amendment recommended treatment with stress-dose steroids before or immediately after injection of vidutolimod for patients with adrenal insufficiency due to an increased risk of moderate to severe AEs, such as hypotension.

End Points and Assessments

The primary objective of the dose-escalation part of this phase Ib study was to determine the recommended phase II dose and schedule of vidutolimod in combination with pembrolizumab. Secondary objectives were to assess the overall safety profile, pharmacodynamic effects, and antitumor activity of vidutolimod plus pembrolizumab.

Safety assessments were performed at baseline and at each vidutolimod dosing visit. All AEs reported were treatment emergent. TRAEs were graded using the National Cancer Institute Common Terminology Criteria for Adverse Events version 5.0 and coded using the Medical Dictionary for Regulatory Activities version 18.1. The relationship of AEs to study treatment was determined by the investigator.

Antitumor activity was determined as best ORR (i.e., percentage of patients with CR or PR), DOR, time to response, and PFS by investigator assessment per RECIST v1.1. Tumor assessments were conducted at screening, every 12 weeks during treatment, and at the end-of-treatment visit. Archival and on-study tumor biopsy samples were collected when possible. Tumor regression in patients who continued study treatment after PD per RECIST v1.1 was assessed by blinded central review according to iRECIST (15).

In Vitro *Cytokine Induction*

Human donor PBMCs were plated at 1.5×10^6 cells/mL and treated with a CpG-A–positive control (2.5 μg/mL; Avecia), G10 (naked CpG-A from vidutolimod; 2.5 μg/mL; BioSpring Biotechnolgie GmbH), vidutolimod (G10+VLP; 10 μg/mL) + anti-Qβ (clone, Qb5; 10 μg/mL), vidutolimod alone (10 μg/mL), anti-Qβ alone (10 μg/mL), a CpG-B–positive control (2006; 2.5 μg/mL; Avecia), a CpG-C agonist (2.5 μg/mL; 5′-TCGAACGTTCGAACGTTCGAACGTTCG AAT-3′ with a phosphorothioate backbone; Avecia), a TLR4 agonist (MPL-A, Enzo Life Sciences, catalog no. ALX-581-205-C100; 200 μg/mL), or a TLR7/8 agonist (R-848, InvivoGen, catalog no. HrlT848; 1.0 μg/mL) for 48 hours (14). Supernatants were collected and analyzed using the Human Cytokine Magnetic 25-Plex Luminex Assay (Thermo Fisher Scientific, catalog no. LHC0009M). Assays were performed in duplicate.

Multiplexed Cytokine Analysis

Serum samples collected at baseline and multiple timepoints after treatment were analyzed using the Human Cytokine Magnetic 25-Plex Luminex Assay (Thermo Fisher Scientific, catalog no. LHC0009M). The assay was performed by QPS, LLC, with samples analyzed in triplicate and read on a Bio-Plex 200 (Bio-Rad Laboratories, Inc.). Concentrations for each biomarker were back-calculated against the corresponding standard curve using a five-parameters logistic regression.

Qβ Antibody Detection

Anti-Qβ development was assessed using an enzyme-linked immunosorbent assay. 96-well plates (Corning, product 3590) were coated with vidutolimod. Serum samples and monoclonal anti-Qβ (clone Qb5) standard were incubated overnight at 4°C, and human antibodies were detected using goat anti-human Ig-HRP (SouthernBiotech, catalog no. 2010-05). Plates were developed with 3,3′,5,5′-tetramethylbenzidine (Sigma-Aldrich, catalog no.T8665), and anti-Qβ concentrations were calculated from the standard curve generated with monoclonal anti-Qβ antibody (clone Qb5l ref. 14).

IHC Analysis

Four-micron-thick serial sections of formalin-fixed paraffin-embedded (FFPE) tumor biopsy tissue were immunostained for CD8 (Dako Agilent, catalog no. M7103) and PD-L1 (Cell Signaling Technology, catalog no. 13684). Slides were stained in a Leica Bond RX Autostainer and scanned on Aperio's AT Turbo and CS brightfield slide scanning systems (Leica Biosystems Inc.). Staining and analysis were performed by Flagship Biosciences.

Full-scan analysis was performed using Flagship Bioscience's proprietary computational tissue analysis (cTA) imaging software system. Digital H-scores ranging from 0 to 300 were calculated using the following standard formula: [3 × % cells +3 intensity] + [2 × % cells +2 intensity] + [1 × % cells +1 intensity].

Next-Generation Sequencing

RNA extraction from baseline and on-treatment tumor FFPE biopsies and RNA sequencing (RNA-seq) were performed by Genewiz. Ribosomal RNA (rRNA) was depleted using the Illumina Ribo-Zero rRNA removal kit (Illumina) and RNA-seq libraries were prepared using the Illumina TruSeq Stranded RNA Library Preparation Kit (Illumina). Single-indexed libraries were pooled and sequenced on the Illumina HiSeq 4000 Sequencing System (2 × 150 bp reads).

Alignment, Processing, and Gene Expression Analysis

RNA-seq data were aligned to the Ensembl human reference transcriptome (GRCh38, Release 94) by HiSat2. Gene expression patterns were assessed across treatment response groups (PD versus CR/PR/SD) and timepoints (baseline versus on-treatment). Gene expression was annotated by Ensembl (Release 94) and summarized by StringTie as fragments per kilobase transcript per million mapped reads (FPKM). Gene expression was normalized as the z-score of the gene expression (FPKM) across all samples and displayed using the ggplot2 R package.

Statistical Analysis

The sample size was based on clinical considerations and a standard 3+3 dose-escalation design. All patients who received ≥1 dose of vidutolimod were included in the intention-to-treat population and evaluated for safety and antitumor activity. Descriptive statistics included means with SD or medians with minimum and maximum values for continuous variables, and counts and percentages for categorical variables. Exact methods (Clopper–Pearson 95% CIs) were used for ORR. Patients who discontinued prior to having a postbaseline follow-up tumor assessment were counted as nonresponders. Median DOR (starting from first evidence of response) and PFS were estimated using the Kaplan–Meier method. Missing data were not imputed. Censoring of DOR and PFS data was based on US Department of Health and Human Services censoring rules. Given the exploratory nature of this study, no adjustments for multiple comparisons were made and no formal comparisons of dose levels were performed for any end points. Analyses were performed with SAS software, version 9.4.

Data Availability

The complete deidentified patient data set will be made available to qualified researchers who provide a methodically sound proposal beginning two years after manuscript publication. Data requests may be sent to admin@checkmatepharma.com. The final study protocol and statistical analysis plan can be shared upon request.

Authors' Disclosures

A. Ribas reports personal fees from Amgen, Chugai, Genentech, Merck, Novartis, Roche, Sanofi and Vedanta, 4C Biomed, Apricity, Arcus, Highlight, Compugen, ImaginAb, MapKure, Merus, Rgenix, Lutris, PACT Pharma, Tango, Advaxis, CytomX, Five Prime, RAPT, Isoplexis, Kite-Gilead, and grants from Agilent, Bristol-Myers Squibb outside the submitted work; in addition, A. Ribas has a patent for US Provisional Patent Application No. 62/794,343 pending. T. Medina reports grants from Merck, Bristol Myers Squibb, Iovance, Regeneron, Nektar, Moderna, Replimune, Seattle Genetics, Bioatla, grants from National Cancer Institute, and grants from Checkmate during the conduct of the study. J.M. Kirkwood reports Amgen, Ankyra Therapeutics, Axio Research/Instil Bio, BMS, Castle Biosciences, Checkmate Pharmaceuticals, DermTech, Elsevier, Harbour BioMed, Immunocore LLC, Iovance Biotherapeutics, Istari Oncology, Merck, Millennium Pharmaceuticals/Takeda Pharmaceutical, Natera Inc., Novartis, OncoCyte Pharmaceuticals, OncoSec Medical Inc., Pfizer, Scopus BioPharma. Y. Zakharia reports Advisory Board: BMS, Amgen, Roche Diagnostics, Novartis, Janssen, Eisai, Exelixis, Castle Bioscience, Array, Bayer, Pfizer, Clovis, EMD serono; grant/research support from: NewLink Genetics, Pfizer, Exelixis, Eisai (institution clinical trial support); DSMC: Janssen Research and Development; consultant honorarium: Pfizer, Novartis. R. Gonzalez reports grants from Checkmate Pharmaceuticals during the conduct of the study; grants from BMS and grants from Merck outside the submitted work. D. Davar reports grants from Checkmate Pharmaceuticals during the conduct of the study; grants from Arcus, grants from Bristol-Myers Squibb, CellSight Technologies, Merck Inc., and grants from Tesaro/GSK outside the submitted work; and US Patent 63/124,231, "Compositions and Methods for Treating Cancer," Dec 11, 2020. US Patent 63/208,719, "Compositions and Methods for Determining Responsiveness to Immune Checkpoint Inhibitors (ICI), Increasing Effectiveness of ICI and Treating Cancer," June 9, 2021. B. Chmielowski reports personal fees from Genentech, IDEAYA, Biothera, Epizyme, Deciphera, OncoSec, Iovance, Sanofi Genzyme, and personal fees from Regeneron outside the submitted work. K.M. Campbell reports grants from Cancer Research Institute and grants from NCI during the conduct of the study; personal fees from Tango Therapeutics, PACT Pharma, and Geneoscopy LLC outside the submitted work. A. Morris reports was employed by Checkmate Pharmaceuticals and owns stock in the company. J.E. Wooldridge reports other support from Checkmate Pharmaceuticals during the conduct of the study; and is an employee of Checkmate Pharmaceuticals, the Sponsor of this work. J.J. Luke reports Scientific Advisory Board: (no stock) 7 Hills, Fstar, RefleXion, Xilio (stock) Actym, Alphamab Oncology, Arch Oncology, Kanaph, Mavu, Onc.AI, Pyxis, Tempest; consultancy with compensation: Abbvie, Alnylam, Bayer, Bristol-Myers Squibb, Checkmate, Crown, Cstone, Eisai, EMD Serono, Flame, Genentech, Gilead, Kadmon, KSQ, Janssen, Immunocore, Inzen, Macrogenics, Merck, Mersana, Nektar, Novartis, Pfizer, Regeneron, Ribon, Rubius, Silicon, Synlogic, TRex, Werewolf, Xencor; research support: (all to institution for clinical trials unless noted) AbbVie, Agios (IIT), Array (IIT), Astellas, Bristol-Myers Squibb (IIT & industry), Corvus, EMD Serono, Fstar, Genmab, Ikena, Immatics, Incyte, Kadmon, KAHR, Macrogenics, Merck, Moderna, Nektar, Numab, Replimmune, Rubius, Spring bank, Synlogic, Takeda, Trishula, Tizona, Xencor; patents: (both provisional) Serial #15/612,657 (Cancer Immunotherapy), PCT/US18/36052 (Microbiome Biomarkers for Anti-PD-1/PD-L1 Responsiveness: Diagnostic, Prognostic and Therapeutic Uses Thereof). G.J. Weiner reports grants from Checkmate Pharmaceuticals during the conduct of the study; in addition, G.J. Weiner has a patent 6,218,371 issued, licensed, and with royalties paid from Checkmate Pharmaceuticals. A.M. Krieg reports other support from Checkmate Pharmaceuticals during the conduct of the study; other support from Checkmate Pharmaceuticals outside the submitted work; in addition, A.M. Krieg has a patent for Checkmate issued. M.M. Milhem reports other support from Novartis, Blueprints Medicine, Immunocore, Amgen, Trieza, Array Biopharma, Biontech, and other support from Exicure outside the submitted work. No disclosures were reported by the other authors.

Authors' Contributions

A. Ribas, J.M. Kirkwood, D. Mauro, G.J. Weiner, and A.M. Krieg contributed to the conception and/or design of the study. A. Ribas, T. Medina, J.M. Kirkwood, H. Kelley, A. Morris, D. Mauro, A.M. Krieg, and M.M. Milhem contributed to the development of the study protocol. A. Ribas, T. Medina, J.M. Kirkwood, Y. Zakharia, R. Gonzalez, D. Davar, B. Chmielowski, R. Bao, J.J. Luke, G.J. Weiner, and M.M. Milhem were involved in data collection. A. Ribas, J.M. Kirkwood, K.M. Campbell, R. Bao, H. Kelley, A. Morris, D. Mauro, J.E. Wooldridge, J.J. Luke, G.J. Weiner, A.M. Krieg, and M.M. Milhem were involved in data analysis. All authors participated in the interpretation of data. All authors were involved in the drafting and revision of the manuscript, and all authors approved the final version of the manuscript for publication.

Acknowledgments

The authors thank the patients and their families and caregivers for participating in this study, and all site personnel. The authors also thank Grace Cherry, NP, for providing pictures of superficial lesions on study, Audrey Folan for statistical programming work to support this manuscript, Sue Blackwell for performing the *in vitro* cytokine induction experiments, and Imaging Endpoints LLC for performing the blinded central review. This study was funded by Checkmate Pharmaceuticals, Inc. A. Ribas was supported by R35 CA197633 and the Parker Institute for Cancer Immunotherapy. K.M. Campbell was supported by the UCLA Tumor Immunology Training Grant (NIH T32CA009120) and the Cancer Research Institute Irvington Postdoctoral Fellowship Program. Editorial support was provided by Steffen Biechele, PhD, of ApotheCom and was funded by Checkmate Pharmaceuticals, Inc.

The publication costs of this article were defrayed in part by the payment of publication fees. Therefore, and solely to indicate this fact, this article is hereby marked "advertisement" in accordance with 18 USC section 1734.

Note

Supplementary data for this article are available at Cancer Discovery Online (http://cancerdiscovery.aacrjournals.org/).

Received April 2, 2021; revised July 9, 2021; accepted July 22, 2021; published first July 29, 2021.

REFERENCES

1. Tumeh PC, Harview CL, Yearly JH, Shintaku IP, Taylor EJM, Robert L, et al. PD-1 blockade induces responses by inhibiting adaptive immune resistance. Nature 2014;515:568–71.
2. Sharma P, Hu-Lieskovan S, Wargo JA, Ribas A. Primary, adaptive, and acquired resistance to cancer immunotherapy. Cell 2017;168:707–23.
3. Cristescu R, Mogg R, Ayers M, Albright A, Murphy E, Yearley J, et al. Pan-tumor genomic biomarkers for PD-1 checkpoint blockade-based immunotherapy. Science 2018;362:eaar3593.
4. Ayers M, Lunceford J, Nebozhyn M, Murphy E, Loboda A, Kaufman DR, et al. IFN-gamma-related mRNA profile predicts clinical response to PD-1 blockade. J Clin Invest 2017;127:2930–40.
5. Fuertes MB, Kacha AK, Kline J, Woo SR, Kranz DM, Murphy KM, et al. Host type I IFN signals are required for antitumor CD8+ T cell responses through CD8{alpha}+ dendritic cells. J Exp Med 2011;208:2005–16.

6. Lombardi VC, Khaiboullina SF, Rizvanov AA. Plasmacytoid dendritic cells, a role in neoplastic prevention and progression. Eur J Clin Invest 2015;45:1–8.
7. Swiecki M, Colonna M. The multifaceted biology of plasmacytoid dendritic cells. Nat Rev Immunol 2015;15:471–85.
8. Krieg AM. CpG still rocks! Update on an accidental drug. Nucleic Acid Ther 2012;22:77–89.
9. Fourcade J, Sun Z, Pagliano O, Chauvin JM, Sander C, Janjic B, et al. PD-1 and Tim-3 regulate the expansion of tumor antigen-specific CD8$^+$ T cells induced by melanoma vaccines. Cancer Res 2014;74:1045–55.
10. Chan MP, Onji M, Fukui R, Kawane K, Shibata T, Saitoh S, et al. DNase II-dependent DNA digestion is required for DNA sensing by TLR9. Nat Commun 2015;6:5853.
11. Alculumbre SG, Saint-Andre V, Di Domizio J, Vargas P, Sirven P, Bost P, et al. Diversification of human plasmacytoid predendritic cells in response to a single stimulus. Nat Immunol 2018;19:63–75.
12. Båve U, Magnusson M, Eloranta ML, Perers A, Alm GV, Rönnblom L. Fc gamma RIIa is expressed on natural IFN-alpha-producing cells (plasmacytoid dendritic cells) and is required for the IFN-alpha production induced by apoptotic cells combined with lupus IgG. J Immunol 2003;171:3296–302.
13. Means TK, Latz E, Hayashi F, Murali MR, Golenbock DT, Luster AD. Human lupus autoantibody-DNA complexes activate DCs through cooperation of CD32 and TLR9. J Clin Invest 2005;115:407–17.
14. Lemke-Miltner CD, Blackwell SE, Yin C, Krug AE, Morris AJ, Krieg AM, et al. Antibody opsonization of a TLR9-agonist–containing viruslike particle enhances in situ immunization. J Immunol 2020; 204:1386–94.
15. Hodi FS, Hwu WJ, Kefford R, Weber JS, Daud A, Hamid O, et al. Evaluation of immune-related response criteria and RECIST v1.1 in patients with advanced melanoma treated with pembrolizumab. J Clin Oncol 2016;34:1510–7.
16. Maude SL, Frey N, Shaw PA, Aplenc R, Barrett DM, Bunin NJ, et al. Chimeric antigen receptor T cells for sustained remissions in leukemia. N Engl J Med 2014;371:1507–17.
17. Blackwell SE, Krieg AM. CpG-A-induced monocyte IFN-gamma-inducible protein-10 production is regulated by plasmacytoid dendritic cell-derived IFN-alpha. J Immunol 2003;170:4061–8.
18. Braun M, Jandus C, Maurer P, Hammann-Haenni A, Schwarz K, Bachmann MF, et al. Virus-like particles induce robust human T-helper cell responses. Eur J Immunol 2012;42:330–40.
19. Ribas A, Dummer R, Puzanov I, VanderWalde A, Andtbacka RHI, Michielin O, et al. Oncolytic virotherapy promotes intratumoral T cell infiltration and improves anti-PD-1 immunotherapy. Cell 2017;170:1109–19.
20. Spranger S, Luke JJ, Bao R, Zha Y, Hernandez KM, Li Y, et al. Density of immunogenic antigens does not explain the presence or absence of the T-cell-inflamed tumor microenvironment in melanoma. Proc Natl Acad Sci U S A 2016;113:E7759–E68.
21. Zimmer L, Apuri S, Eroglu Z, Kottschade LA, Forschner A, Gutzmer R, et al. Ipilimumab alone or in combination with nivolumab after progression on anti-PD-1 therapy in advanced melanoma. Eur J Cancer 2017;75:47–55.
22. Ribas A, Kirkwood JM, Flaherty KT. Anti-PD-1 antibody treatment for melanoma. Lancet Oncol 2018;19:e219.
23. Pires Da Silva I, Ahmed T, Lo S, Reijers ILM, Weppler A, Betof Warner A, et al. Ipilimumab (IPI) alone or in combination with anti-PD-1 (IPI+PD1) in patients (pts) with metastatic melanoma (MM) resistant to PD1 monotherapy. J Clin Oncol 2020;38:10005.
24. Brody JD, Ai WZ, Czerwinski DK, Torchia JA, Levy M, Advani RH, et al. In situ vaccination with a TLR9 agonist induces systemic lymphoma regression: a phase I/II study. J Clin Oncol 2010;28:4324–32.
25. Ribas A, Medina T, Kummar S, Amin A, Kalbasi A, Drabick JJ, et al. SD-101 in combination with pembrolizumab in advanced melanoma: results of a phase Ib, multicenter study. Cancer Discov 2018;8:1250–7.
26. Sabree SA, Voigt AP, Blackwell SE, Vishwakarma A, Chimenti MS, Salem AK, et al. Direct and indirect immune effects of CMP-001, a virus-like particle containing a TLR9 agonist. J Immunother Cancer 2021;9:e002484.
27. Babiker HM, Subbiah V, Ali A, Algazi A, Schachter J, Lotem M, et al. Tilsotolimod engages the TLR9 pathway to promote antigen presentation and Type-I IFN signaling in solid tumors [abstract]. In: Proceedings of the AACR Annual Meeting 2020; 2020 Apr 27–28 and 2020 June 22–24 (Virtual Meeting); Philadelphia, PA. Abstract CT134.